On the simulation of turbulent precipitation in a tubular reactor via computational fluid dynamics

ON THE SIMULATION OF TURBULENT PRECIPITATION
IN A TUBULAR REACTOR VIA COMPUTATIONAL FLUID DYNAMICS

D.L. Marchisio, R.O. Fox, A.A. Barresi, M. Garbero and G. Baldi

paper 55. CD-ROM Edition, pp. 486-494

International Scientific Committee *Comité Scientifique*

chairmen Joël BERTRAND, France
Lionel CHOPLIN, France

members Edmundo BRITO DE LA FUENTE, Mexico
Arthur W. ETCHELLS, USA
David FLETCHER, Australia
Ivan FORT, Czeck Republic
Yushi HIRATA, Japan
Frank JEURISSEN, The Netherlands
Franco MAGELLI, Italy
Alvin NIENOW, UK
Vivek RANADE, India
Anders RASMUSON, Sweeden
Jean-Louis SALAGER, Venezuela
PhilippeTANGUY, Canada
Catherine XUEREB, France

Organizing Committee *Comité d'Organisation*

Marion ALLIET, Toulouse, France
Jack LEGRAND, St Nazaire, France
Nathalie LE SAUZE, Toulouse, France
H.Z. LI, Nancy, France
Paul MAVROS, Thessalonique, Grèce
Martine POUX, Toulouse, France

Coordinators *Coordination*

Joël BERTRAND, LGC, Toulouse, France
e-mail : Joel.Bertrand@ensiacet.fr
Lionel CHOPIN, GEMICO, Nancy, France
e-mail : Lionel.Choplin@ensic.u-nancy.fr

Contact - Information

PROGEP
Florence FOUCAUD
18 chemin de la Loge
31078 Toulouse Cedex 4
phone : +33 (0)5 62 25 23 80 - +33 (0)5 62 26 07 36
fax : +33 (5) 62 25 23 18
e-mail : progep@ensiacet.fr
http://www.ensiacet.fr/PROGEP/

International Symposium on Mixing in Industrial Processes - ISMIP4
14-16 May 2001 - Toulouse (France)

ON THE SIMULATION OF TURBULENT PRECIPITATION IN A TUBULAR REACTOR VIA COMPUTATIONAL FLUID DYNAMICS

D.L. MARCHISIO (1), R.O. FOX (2), A.A. BARRESI (1), M. GARBERO (1) and G. BALDI (1)

- (1) Dip. Scienza dei Materiali ed Ingegneria Chimica
  Politecnico di Torino
  C.so Duca degli Abruzzi 24, Torino
  10129 ITALY
  e-mail : marchis@athena.polito.it

- (2) Dep. Chemical Engineering
  Iowa State University
  2114 Sweeney Hall, Ames
  IA 50011, USA
  e-mail : rofox@iastate.edu

Abstract. Precipitation of barium sulphate from aqueous solutions was investigated in a tubular reactor. Crystal size distribution and morphology were measured at the reactor outlet. Experimental data were compared with model predictions using CFD coupled with a micromixing model. Some anti-symmetric effects of ion excess on precipitation were studied and activity coefficients were used in modeling precipitation. Results show that thermodynamic properties of solutions plays a role in determining nucleation and growth rates but this approach alone is not sufficient to give satisfactory agreement.

Key-words. CFD, micromixing, finite-mode pdf, precipitation, barium sulphate, tubular reactor.

INTRODUCTION

Computational Fluid Dynamics (CFD) is an emerging tool for reactor performance prediction, design and scale up. The use of this technique is particularly useful for studying mixing-controlled reactions, in which accurate knowledge of the flow field and turbulent properties is of primary importance. Precipitation of sparingly soluble salts is one of these cases. The influence of mixing on crystal size distribution (CSD) and morphology has been investigated by various authors, yielding different and sometimes contradictory results. Barium sulphate precipitation from aqueous solutions is one of the most common test reactions used in this field. In past years this reaction has been used to validate micromixing models (Pohorecki and Baldyga, 1983; Garside and Tavare, 1985; David and Marcant, 1994; Baldyga et al., 1995) and all disagreement between simulations and experiments were attributed to the use of simple mechanistic models. The use of CFD has helped in gathering a huge amount of information concerning local flow field properties and has provided a profitable way for modeling turbulent reacting flows. Moreover, application to barium sulphate precipitation (Baldyga and Orciuch, 1999; Marchisio *et al.*, 2000a) has shown that not always does micromixing play a crucial role, confirming what has been found by Brucato *et al.* (2000) in another reacting case for a stirred tank reactor.

Thanks to the better understanding of mixing dynamics, the idea of incorporating more realistic kinetics rather than more realistic micro-mixing models, has become more plausible. Recent experimental results have shown that kinetic expressions available in literature need to be improved in order to take into account some non-stoichiometric effects and that the precipitation model needs to include the effect of aggregation.

Concerning the first point Aoun *et al.* (1996) supposed that in barium sulphate precipitation the effect of non-stoichiometric conditions was extremely important and quantified this effect in terms of the ratio of the reactant concentrations. Phillips *et al.* (2000) working with a single-feed semi-batch reactor

investigated the effect of the stoichiometric ratio and showed the inability of the kinetic expressions to provide reasonable results in these operating conditions. The effect of ion excess on CSD and morphology during barium sulphate precipitation has been recently investigated by Wong *et al.* (2000) who found results in contradiction with what was found by Aoun *et al.* (1996). In fact, they did not observe symmetrical size trends on both sides of the stoichiometric plane (i.e., working either with an excess of barium or of sulphate ions). Concerning the role of aggregation during precipitation, experimental results at high supersaturation show a strong aggregation rate that causes disagreement with model predictions (Baldyga and Orciuch, 1999; Phillips *et al.*, 2000). Marchisio *et al* (2000b) modeling a tubular reactor with coaxial feeds showed that also in dilute systems aggregation of nuclei and microcrystals takes place and proposed a simple approach to include it in the precipitation model using constant aggregation kernels.

The aim of this work is to model turbulent precipitation in a tubular reactor using CFD, and to compare experimental data with model predictions. In this work we focused our attention on this non-symmetric effect between barium and sulphate ions, whereas the role of aggregation will be the object of our future work.

PRECIPITATION MODEL

Using CFD macro- and meso-scale mixing are modeled by the turbulence model. In order to take into account also mixing at the molecular level a micromixing model must be coupled. In this work a finite-mode probability density function (FMPDF) approach was used (Fox, 1998; Marchisio *et al.*, 2000a). This approach has been shown to work with good accuracy with small computational effort, as compared with a full pdf method, and moreover comparison with other models available in the literature has been investigated (Piton et al., 2000). Using this approach the PDF of all scalars is represented by a finite set of delta functions and if the first scalar is the mixture fraction (ξ), the presumed PDF has the following form:

$$f(\xi;x,t) = \sum_{n=1}^{Ne} p_n(x,t)\,\delta\left(\xi - \langle\xi\rangle_n(x,t)\right) \tag{1}$$

where N_e is the number of modes and p_n is the probability of the mode n. Taking N_e=3 the system can be thought as constituted by three environments. The first Environment corresponds to the first stream entering into the reactor ($\langle\xi\rangle_1$=1), the second Environment corresponds to the second stream entering the reactor ($\langle\xi\rangle_2$=0), while the third corresponds to the Environment in which the two inlet streams are mixed together and react. The three environments (mode) probabilities are defined by their scalar transport equations

$$\frac{\partial p_1}{\partial t} + \frac{\partial}{\partial x_i}\left(\langle u_i\rangle p_1\right) = \frac{\partial}{\partial x_i}\left(\Gamma_t \frac{\partial p_1}{\partial x_i}\right) + \gamma_s p_3 - \gamma p_1(1-p_1) \tag{2}$$

$$\frac{\partial p_2}{\partial t} + \frac{\partial}{\partial x_i}\left(\langle u_i\rangle p_2\right) = \frac{\partial}{\partial x_i}\left(\Gamma_t \frac{\partial p_2}{\partial x_i}\right) + \gamma_s p_3 - \gamma p_2(1-p_2) \tag{3}$$

where $p_3 = 1 - p_1 - p_2$, and the transport equation for the weighted mixture fraction in Environment 3 ($s_3=\langle\xi\rangle_3 p_3$) is defined as follows

$$\frac{\partial s_3}{\partial t} + \frac{\partial}{\partial x_i}\left(\langle u_i\rangle s_3\right) = \frac{\partial}{\partial x_i}\left(\Gamma_t \frac{\partial s_3}{\partial x_i}\right) - \gamma_s p_3\left(\langle\xi\rangle_1 + \langle\xi\rangle_2\right) + \gamma p_1(1-p_1)\langle\xi\rangle_1 + \gamma p_2(1-p_2)\langle\xi\rangle_2 \tag{4}$$

where $\langle\xi\rangle_1$=1, $\langle\xi\rangle_2$=0, Γ_t is the turbulent diffusivity, $\langle u_i\rangle$ is the Reynolds averaged velocity in the i direction, and γ and γ_s are respectively the micromixing rate and the spurious dissipation rate:

$$\gamma = C_\phi \frac{\varepsilon}{k} \frac{\langle\xi''^2\rangle}{\left[p_1(1-p_1)(1-\langle\xi\rangle_3)^2 + p_2(1-p_2)\langle\xi\rangle_3^2\right]} \tag{5}$$

$$\gamma_s = \frac{2\Gamma_t \frac{\partial\langle\xi\rangle_3}{\partial x_i}\frac{\partial\langle\xi\rangle_3}{\partial x_i}}{1-2\langle\xi\rangle_3(1-\langle\xi\rangle_3)} \tag{6}$$

where ε and k are respectively the turbulent dissipation rate and the turbulent kinetic energy, C_ϕ is a constant of order of unity and $\langle\xi^2\rangle$ is the mixture fraction variance that it is defined by

$$\langle\xi^2\rangle = p_1 + s_3^2/p_3 - (p_1 + s_3)^2 \tag{7}$$

The spurious dissipation (χ) is a correction term, deriving from the finite mode representation, whereas the micromixing term (γ) is due to molecular mixing. These two parameters have been determined in order to ensure that the mixture fraction variance obeys the correct transport equation.

The population balance was solved in terms of the moments of the CSD leading to a set of differential equations:

$$\frac{\partial m_j}{\partial t} + \frac{\partial}{\partial x_i}\left(\langle u_i\rangle m_j\right) = \frac{\partial}{\partial x_i}\left(\Gamma_t \frac{\partial m_j}{\partial x_i}\right) + B\left(\langle c_A\rangle_3, \langle c_B\rangle_3\right) + j m_{j-1} G\left(\langle c_A\rangle_3, \langle c_B\rangle_3\right) \tag{8}$$

where B is the nucleation rate, G is the growth rate, m_j is the mean value of the j^{th} moment of the particle number density function (i.e., $m_j = p_3 \langle m_j\rangle_3$), $\langle c_A\rangle_3$ and $\langle c_B\rangle_3$ are the local reactant concentrations in Environment 3 that can be calculated introducing the reaction progress variable (Y)

$$\frac{\langle c_A\rangle_3}{c_{Ao}} = \frac{s_3 - \xi_s\langle Y\rangle}{p_3}, \qquad \frac{\langle c_B\rangle_3}{c_{Bo}} = \frac{p_3 - s_3 - (1-\xi_s)\langle Y\rangle}{p_3} \tag{9}$$

$$\frac{\partial\langle Y\rangle}{\partial t} + \frac{\partial}{\partial x_i}\left(\langle u_i\rangle\langle Y\rangle\right) = \frac{\partial}{\partial x_i}\left(\Gamma_t \frac{\partial\langle Y\rangle}{\partial x_i}\right) + \frac{\rho\beta k_v m_2 G}{\xi_s c_{Ao} M} \tag{10}$$

where c_{Ao} and c_{Bo} are the inlet reactant concentrations, ρ is the crystal density, k_v is the crystal shape factor, and M is the crystal molecular weight and

$$\xi_s = \frac{c_{Bo}}{c_{Ao} + c_{Bo}} \tag{11}$$

The mean crystal size can be calculated using the following expression

$$L_{43} = \frac{m_4}{m_3} \tag{12}$$

Introducing the moments of the crystal size distribution, a nine scalars model is obtained that can be implemented in FLUENT as user defined scalars as described by Piton *et al.* (2000).

PRECIPITATION KINETICS AND SHAPE FACTORS

Barium sulphate precipitation is a well-known reaction, for which several kinetics are available in literature. A complete review of a number of kinetic expressions available in literature can be found in Aoun *et al.* (1999). Most kinetics are obtained from the experimental work of Nielsen (Nielsen, 1964; Nielsen, 1984; Nielsen and Toft, 1984). The nucleation rate can be expressed with the following equation:

$$B(c_A, c_B) = \begin{cases} 2.83\times10^{10}\left(\sqrt{c_A c_B} - \sqrt{k_s}\right)^{1.775}\ (1/m^3 s) & for \quad \sqrt{c_A c_B} - \sqrt{k_s} < 10\ mol/m^3 \\ 2.53\times10^{-3}\left(\sqrt{c_A c_B} - \sqrt{k_s}\right)^{9.5}\ (1/m^3 s) & for \quad \sqrt{c_A c_B} - \sqrt{k_s} > 10\ mol/m^3 \end{cases} \tag{13}$$

in which two regions are described, one for homogeneous nucleation and one for heterogeneous nucleation (Baldyga *et al.*, 1995). For crystal growth a two steps model can be used to evaluate the growth rate as a function of reactant concentrations:

$$G(c_A, c_B) = k_r\left(\sqrt{c_{As}c_{Bs}} - \sqrt{k_s}\right)^2 = k_d(c_A - c_{As}) = k_d(c_B - c_{Bs}) \quad (m/s) \tag{14}$$

where c_A and c_B are the concentrations in the bulk whereas c_{As} and c_{Bs} are the concentrations on the crystal surface where a surface reaction occurs, whose constant has been found by Nielsen (1984) to be equal to 5.8×10^{-8} (m/s)/(mol/m^3)^2. Nagata (1975) found that the mass transfer coefficient (k_d) reaches a constant value at about 10 μm of particle size and is kept nearly constant for particles smaller than 10 μm,

notwithstanding the difference in solute. According to this theory k_d has been fixed by Baldyga *et al.* (1995) to fall in the range between 10^{-7}-10^{-8} (m/s)/(mol/m^3).

More recent results in the field of mass transfer to microparticles (Armenante and Kirwan, 1989) showed that also for microparticles in agitated system the theoretical limit of Sherwood number equal to 2 is valid. Under this assumption the mass transfer coefficient is size-dependent and can be calculated using the following expression

$$k_d = \frac{ShDM}{d_p \rho} \tag{15}$$

where D is the molecular diffusivity, M is the molecular weight, d_p is the particle diameter (i.e., L_{43}) and ρ is the particle density. From this equation it comes that for particles smaller than 1 μm, the mass transfer coefficient is bigger than 10^{-7}.

These equations were derived under the assumption of ideal thermodynamic behavior of the solution. Bromley (1973) investigated the thermodynamic properties of strong electrolytes in aqueous solutions and found that for multi-component salt solutions, ignoring interactions between like charged species, the following equation for calculating the activity coefficient ($\gamma_\pm$) is applicable:

$$\log \gamma_\pm = \frac{-2.044 \cdot \sqrt{I}}{1+\sqrt{I}} + \left(\frac{F_1}{2} + \frac{F_2}{2} \right) \tag{16}$$

where I is the total ionic strength of the solution, and F_1 and F_2 take into account ions interactions. Starting from the work of Wei and Garside (1997) that introduced activity coefficients, the following growth rate expression can be found:

$$G(c_A, c_B) = 4.0 \times 10^{-8} \left(\sqrt{c_{As} c_{Bs}}\, \gamma_\pm - \sqrt{k_s} \right)^2 = k_d (c_A - c_{As}) = k_d (c_B - c_{Bs}) \quad (m/s) \tag{17}$$

Using the form of Eq.13 also for nucleation rate it is possible to find a new expression:

$$B(c_A, c_B) = \begin{cases} 6.61 \times 10^{10} \left(\sqrt{c_A c_B}\, \gamma_\pm - \sqrt{k_s} \right)^{2.71} \left(1/m^3 s \right) & for \quad \sqrt{c_A c_B}\, \gamma_\pm - \sqrt{k_s} < 4.27\ mol/m^3 \\ 3.60 \times 10^{-4} \left(\sqrt{c_A c_B}\, \gamma_\pm - \sqrt{k_s} \right)^{24.9} \left(1/m^3 s \right) & for \quad \sqrt{c_A c_B}\, \gamma_\pm - \sqrt{k_s} > 4.27\ mol/m^3 \end{cases} \tag{18}$$

This equation was found by forcing the birth rate to agree with experimental data by Nielsen. Shape factors were partially taken from a previous work and in part recalculated in this work using new experimental data. However it should be highlighted that experimental evidence showed that barium sulphate crystals are almost always flat and thus very far from spherical. In this condition the mean crystal size measured by a laser particles sizer, whose data treatment is based on spherical particles, should be always verified. Results confirmed what previously found (Pagliolico *et al.*, 1999) that the mean crystal size indicated by the particle sizer (d_{43}) is very close to the width of the crystals. Starting from this result, shape factors (k_V^*, k_A^*) can be expressed in terms of this real dimension

$$A = k_A^* d_{43}^2, \tag{19}$$

$$V = k_V^* d_{43}^3. \tag{20}$$

Because the population balance works in terms of a unique characteristic dimension (L_{43}), as explained by Randolph and Larson (1988), it is possible to define new shape factors (k_V, k_A) in terms of the latter, forcing the ratio k_A/k_V to be equal to 6 (i.e., equi-dimensional growth):

$$A = k_A L_{43}^2 \tag{21}$$

$$V = k_V L_{43}^3 \tag{22}$$

Then the relationships between the two notations is as follows:

$$k_V = \frac{1}{k_V^{*2}} \left(\frac{k_A^*}{6} \right)^3 \tag{23}$$

$$k_A = 6 k_V \tag{24}$$

$$d_{43} = 6 \left(\frac{k_V^*}{k_A^*} \right) L_{43} = \phi_C L_{43} \tag{25}$$

Using an average value for all morphologies observed results in:

$k_V = 5; k_A = 30; \phi_C = 3.0$

This value was used to carry out all simulations and the comparison between experimental data and model predictions was done transforming the mean crystal size according to Eq.25.

EXPERIMENAL SET-UP, OPERATING CONDITIONS AND COMPUTATIONAL DETAILS

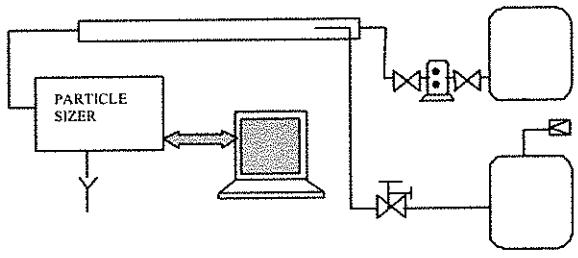

Fig. 1. Experimental set-up

Barium sulphate precitation was studied in a tubular reactor (Fig. 1). Barium chloride and sodium sulphate were alternatively fed in the jet (A) and in the coaxial region (B) and the reactants ratio ($\alpha = c_{Bo}/c_{Ao}$) was varied between 0.01 and 3. The tubular reactor, including the connection, is 2.1 m long and has an internal diameter of 1 cm. The jet is positioned on the reactor axis, with a small pipe of 1 mm internal diameter and 1.5 mm outer diameter. The velocity in the jet was varied keeping the velocity in the coaxial region at 1 m/s, so that the macroscopic Reynolds number was about 10,000. The velocity ratio (VR) between the jet and coaxial flow was varied between 0.5 and 2. The reactor outlet was connected to a laser particle sizer (Coulter LS 230) for on-line measurements (fluid cell). In order to gather information on the total particle number density and the reaction yield, samples were taken from the reactor outlet and gently agitated for 30 minutes. During this period the mean crystal size was monitored using the same particle sizer in another configuration (small volume cell). Measurements were complicated by particle deposition on the particle sizer lens. In order to minimize deposition the measurement time was reduced to 15 seconds and after each run the reactor walls and particle sizer lens were mechanically cleaned. The main difficulty stands in the fact that particles deposited can add further scattering, altering measurements. Thus to ensure that no interaction occurred during measurements, after cleaning the cell with pure water and before the mechanical particles removal, "blank" measurements were carried out. Results show that there is small overlapping between the CSD of deposited particles and particles transported by the flow. Moreover, as a final proof of the validity of this experimental procedure samples from the reactor outlet were taken and immediately filtered avoiding further growth. Filtered particles were analyzed with a Scanning Electron Microscope (SEM) and results were compared with the CSD of the laser particle sizer. Each experiment was repeated 5-6 times and results were statistically treated in order to deal with the poor reproducibility typical of precipitation.

Flow field simulations were carried out with FLUENT (release 5.2) using the standard k-ε model with standard wall functions. Different grids were used in order to reach a grid-independent solution. The final grid size was 130-55 (8416 nodes of live cells), and finer resolution was used near the injection point. Steady-state simulations were carried out under the assumption of axial-symmetry on one half of the reactor geometry (using symmetrical boundary conditions on the reactor axis). The precipitation model was introduced using FLUENT user-defined scalars. First the flow field was solved, and eventually Eqs. 2-4 and Eqs. 8-10 were solved. Under-relaxation factors were decreased while increasing concentration, starting from 1 (no under-relaxation) down to 0.8 for the highest concentration. Simulations were carried out with and without activity coefficients. Assuming that micromixing is important only in the first part of the experiment, using a simple well-mixed approach, precipitation was modeled until reaction was complete (30 minutes). Outlet values of scalars obtained using CFD were used as initial conditions for the well-mixed simulations. Then the reacting system was modeled using CFD coupled with the FMPDF model for the first part, and assuming the system to be perfectly macro- and micro-mixed for the second part. This allowed us to compare also the capability of the model to predict the particle number density. Results were compared with experimental data. Because of the uncertainty in the choice of k_d a parametric investigation in the range between 10^{-7}-10^{-5} (m/s)/(mol/m^3) was carried out. According to Armentante and Kirwan (1988) k_d is size dependent, and McGraw (1997) showed how is possible to handle this kind of growth laws using quadrature method of moments, but in order to simplify the problem a constant value was used. For the well-mixed simulation the usual value [$k_d = 10^{-7}$ (m/s)/(mol/m^3)] was used.

RESULTS AND DISCUSSION

Effect of micromixing

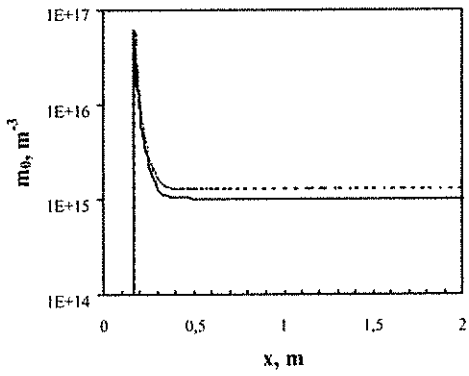

Fig.2. Axial profile of the particle number density on the reactor axis (Re=10,000; VR=1; c_{A_0}=34.101 mol/m^3; c_{B_0}=100 mol/m^3). Solid line: with micromixing model; dotted line: without.

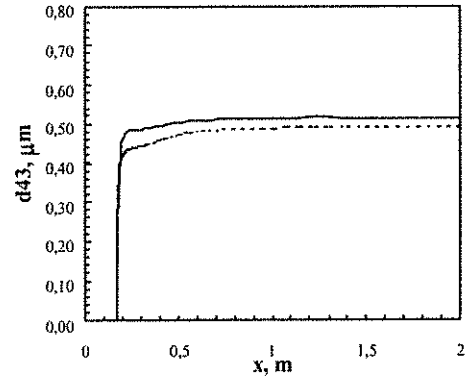

Fig.3. Axial profile of the mean crystal size on the reactor axis (Re=10,000; VR=1; c_{A_0}=34.101 mol/m^3; c_{B_0}=100 mol/m^3). Solid line: with micromixing model; dotted line: without.

In Figs. 2-3 the axial profile of particle number density and mean crystal size, calculated with and without the micromixing model, are reported. In general for these operating conditions the effect of micromixing has been found to be lower than expected. The particle number density shows a peak near the injection zone, whereas far from this point the particle number density decreases due to turbulent diffusion. In this case reaction is complete at the reactor outlet, in fact both the particle number density and the mean crystal size have flat profiles. Neglecting micromixing the particle number density is higher due to fast mixing that overestimates the nucleation rate. The mean crystal size increases and reaches a lower value neglecting micromixing due to higher final particle number density. Overall, the effect of micromixing was almost always appreciable, but model predictions with and without micromixing model were quite similar.

Effect of the reactant concentration ratio

The jet concentration was kept at a fixed value (c_{A_0}=34.101 mol/m^3), whereas the main flow concentration was increased from 0.34 to 100 mol/m^3. Reactants were fed in configuration AB (barium chloride in the jet, sodium sulphate in the main flow) and in configuration BA (vice versa). In Fig. 4 experimental data are reported. Error bars refer to two standard deviations calculated from a basis of 5-6 runs. As it is possible to see in configuration BA particles are smaller and present a quite good reproducibility. Both curves present a weak maximum. This maximum can be explained in terms of the reaction yield, in fact the points in the graph refer to the same amount of reagent in the jet, that is the limiting reactant. Increasing the co-reactant concentration, mean crystal size increases, until reaction is complete. From this point a further increase in co-reactant concentration causes a decreasing trend. In fact, in this range increasing the concentration, nucleation produces more particles at the expense of the same amount of limiting reactant. This causes the formation of more particles but with smaller size. In the same figure a comparison with model predictions is presented. Predictions

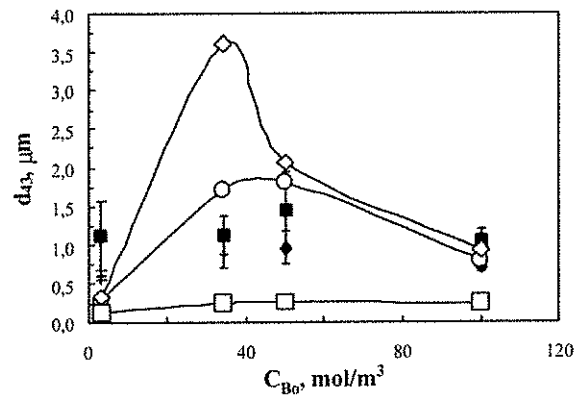

Fig.4. Effect of the reactant concentration ratio (Re=10,000; VR=1; c_{A_0}=34.101 mol/m^3). ■: experimental data (AB); ◆: experimental data (BA); model predictions using Eqs. 13-14, k_d=10^{-7} (m/s)/(mol/m^3); ○ k_d=10^{-6} (m/s)/(mol/m^3); ◊ k_d=10^{-5} (m/s)/(mol/m^3)

refer to simplified kinetics without activity coefficient (Eqs. 13 and 14) for three values of k_d [10^{-7}, 10^{-6}, 10^{-5} (m/s)/(mol/m^3)]. These three values were calculated using Eq. 15 and assuming an average mean crystal size, between reactor inlet and outlet, of about 1, 0.1, 0.01 μm, respectively. As it is possible to see k_d=10^{-6} (m/s)/(mol/m^3) (i.e., L_{43}=0.1 μm) gives the best agreement with experimental data, and hereinafter this value is used. In all cases the model predicts the maximum but we have to highlight that the model is perfectly symmetric and it is not able to predict the difference observed in configuration AB and BA.

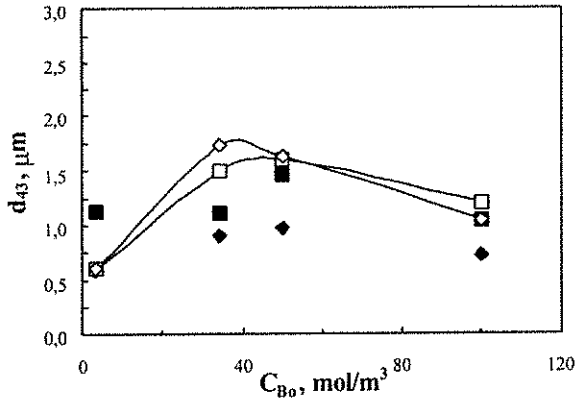

Fig.5. Effect of the reactant concentration ratio (Re=10,000; VR=1; c_{A_0}=34,101 mol/m^3). ■: experimental data (AB); ◆: experimental data (BA); □: model prediction (AB); ◊: model prediction (BA).

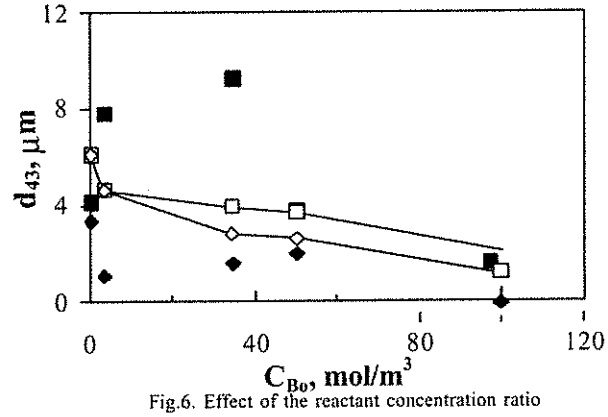

Fig.6. Effect of the reactant concentration ratio on the final mean crystal size after 30 minutes (Re=10,000; VR=1; c_{A_0}=34,101 mol/m^3). ■: experimental data (AB); ◆: experimental data (BA); □: model prediction (AB); ◊: model prediction (BA).

Using Eqs. 16 and 17 the results reported in Fig. 5 were obtained. In this case model predictions at low concentration (when the reaction is not complete) give an opposite effect of the feeding mode, whereas at high concentrations the effect is correctly predicted. Introducing activity coefficients the driving force is reduced by $\gamma_\pm$, and simulations show that an addiction of sodium sulphate reduces $\gamma_\pm$ more than an equal amount of barium chloride. Thus when sodium sulphate is in excess (i.e, it is fed in the main flow) the activity coefficient is smaller. When reaction is not complete this reduction is observed only in the growth rate, resulting in smaller particles. But when reaction is complete the smaller nucleation rate prevails, yielding less particles but with bigger size.

In Fig. 6 the final mean crystal size, after 30 minutes of gentle agitation, is reported, and compared with model predictions. In configuration AB the curves show a maximum located at c_{B_0}=34,101 mol/m^3. The cause for this maximum might be one of two possibilities. Increasing the co-reactant concentration and keeping the jet concentration at the same value, an excess is introduced in the system, affecting the final thermodynamic condition through the solubility product, and moreover the change in morphology observed near this point might influence the mean crystal size. In fact using the specific shape factor for each point of the graph the maximum was predicted but still the agreement was not very good. However, in order to have a fully predictive tool, shape factors were determined by averaging over several morphologies, then a unique shape factor for all runs was used. Although the maximum was not predicted, activity coefficients have been shown to be able to distinguish between the two cases, giving reasonably good agreement with experimental data, especially at higher concentrations. The inlet concentration also affects crystal morphology. In fact increasing this parameter growth rate control moves from the surface reaction region to the diffusion region. In Fig. 7a-b two different morphologies are presented at c_{B_0}=0.34101 and 50 mol/m^3. As it is possible to see at low concentration crystals are well-defined rectangular shaped and increasing concentration crystals become dendritic.

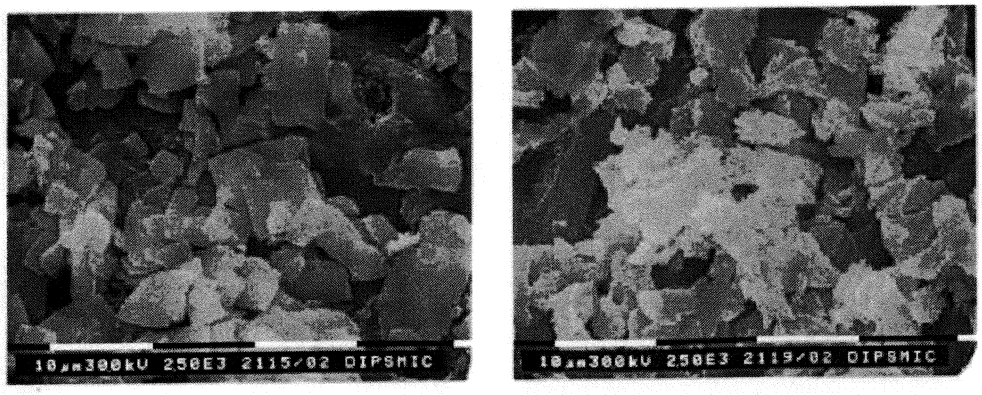

Fig. 7. Morphologies observed for barium sulphate (Re=10,000; VR=1; c_{Ao}=34.101 mol-m^3); (a) left: c_{Bo}=0.34101 mol/m^3; (b) right: c_{Bo}=50.0 mol/m^3.

Effect of the velocity ratio (VR)

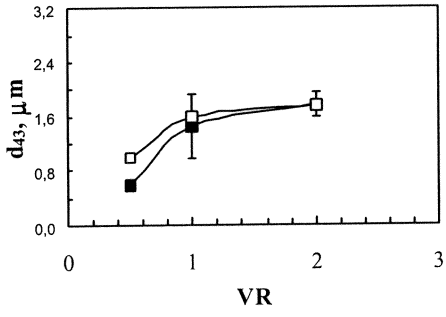

Fig.8. Effect of the velocity ratio on the mean crystal size at the reactor outlet (Re=10,000; c_{Ao}=34.101 mol/m^3; c_{Bo}=100 mol/m^3). : CFD predictions with Eqs. 13-14; ■: experimental data

The effect of the velocity ratio (VR) was studied in the range 0.5 to 2. The velocity of the main flow was kept constant (1 m/s) whereas the jet velocity was varied between 0.5 to 2 m/s. Experiments and simulations were carried out in the configuration AB (barium chloride in the jet, sodium sulphate in the main flow) with an inlet concentration of c_{Ao}=34.101 and c_{Bo}=50 mol/m^3. As it is possible to see in Fig. 8, the effect of VR is to increase the mean crystal size. In fact, by increasing the jet velocity more limiting reactant is added at the same concentration, allowing crystals to grow more. In this case model predictions with and without activity coefficients give very similar results.

ACKNOWLEDGEMENTS

This work has been partially supported by an Italian National research project (MURST 40% Multiphase reactor). Authors gratefully acknowledge Prof. Jerzy Baldyga for his detailed and incisive comments about the use of activity coefficients.

REFERENCES

Aoun, M., Plasari, E., David, R., and J. Villermaux, 1996, "Are barium sulphate kinetics sufficiently known for testing precipitation reactor models?," *Chem. Eng. Sci.*, **51**, 2449.

Aoun, M., Plasari, E., David, R., and J. Villermaux, 1999, "A simultaneous determination of nucleation and growth rates from batch spontaneous precipitation," *Chem. Eng. Sci.*, **54**, 1161.

Armentante, P.M., D.J. Kirwan, 1989, "Mass transfer to microparticles in agitated system," *Chem. Eng. Sci.*, **44**, 2796.

Baldyga, J., and W. Orciuck, 1999, "Barium sulphate precipitation in a pipe - an experimental study and CFD modelling," *Proceeding of the 14th Symposium on Industrial Crystallization*, 12-16 Sept, paper 86, Rugby, UK, 1069.

Baldyga, J., Podgorska, W., and R. Pohorecki, 1995, "Mixing-precipitation model with application to double feed semi-batch precipitation," *Chem. Eng. Sci.*, **50**, 1281.

Bromley, L.A., 1973, "Thermodynamic properties of strong electrolytes in aqueous solutions," *AIChE J.*, **19**, 313.

Brucato, A., Ciofalo, M., Grisafi, F., and R. Tocco, R., 2000, "On the simulation of stirred tank reactor via computational fluid dynamics," *Chem. Eng. Sci.*, **55**, 291.

David, R., and B. Marcant, 1994, "Prediction of micromixing effects in precipitation: case of double-jet precipitator," *AIChE J.*, **40**, 424.

Fox, R.O., 1998, "On the relationship between Lagrangian micromixing models and computational fluid dynamics," *Chem. Eng. Proc.*, **37**, 521.

Garside, J., and N.S. Tavare, 1985, "Mixing reaction and precipitation limits of micromixing in an MSMPR crystalizers," *Chem. Eng. Sci.*, **40**, 1485.

Marchisio, D.L., Fox, R.O., and A.A. Barresi, 2000a, "Simulation of turbulent precipitation in a semi-batch Taylor-Couette reactor using CFD," *AIChE J.*, in press.

Marchisio, D.L., Fox, R.O., Barresi, A.A, and G. Baldi, 2000b, "A CFD approach to study the local importance of aggregation in precipitation," *Proceeding of the 7th International Conference on Multiphase Flow in Industrial Plants*, 13-15 Sept, Bologna, Italy, 363.

McGraw, R., 1997, "Description of aerosol dynamics by the quadrature methods of moments," *Aerosol Science and Technology*, **27**, 255.

Nagata, S., 1975, *Mixing - principles and applications*, Kodansha LTD, Tokyo,

Nielsen, A.E., 1964, *Kinetics of precipitation*, Pergamon Press, London.

Nielsen, A.E., 1984, " Electrolyte crystal growth mechanism," *J. Crystal Growth*, **67**, 289.

Nielsen, A.E., and J.M. Toft, 1984, " Electrolyte crystal growth kinetics," *J. Crystal Growth*, **67**, 278.

Pagliolico, S., Marchisio, D., and A.A. Barresi, 1999, "Influence of operating conditions on $BaSO_4$ crystal size and morphology in a continuous Couette precipitator," *J. Therm. Anal. Cal.*, **56**, 1423.

Phillips, R., Rohani, S., and J. Baldyga, 1999, "Micromixing in a single-feed semi-batch precipitation process," *AIChE J.*, **45**, 82.

Piton, D., Fox, R.O., and B. Marcant, 2000, "Simulation of fine particle formation by precipitation using computational fluid dynamics," *Can. J. Chem. Eng.*, in press.

Pohorecki, R., and J. Baldyga, 1983, "The use of a new micromixing model for determination of crystal size in precipitation," *Chem. Eng. Sci.*, **38**, 79.

Randolph, A.D., and M.A. Larson, 1988, *Theory of particulate process*, 2nd Ed., Academic Press, San Diego.

Wei, H., and J. Garside, 1997, "Application of CFD modelling of precipitation systems," *Trans IChemE*, **75A**, 219.

Wong., D.C.Y., Jaworski, J., and A.W. Nienow, 2000, "Effect of ion excess on particle size and morphology during barium sulphate precipitation: an experimental study," *Paper presented at ISCRE 16*, 10-13 Sept, Cracow, Poland.